# DISCRETE DUALITY FINITE VOLUME APPLIED TO SOIL EROSION

**J. Lakhlili, C. Galusinski, F. Golay**

**IMATH, Université de Toulon, avenue de l'université, BP20132, 83957 La Garde, France**

**Abstract**

This study focuses on the numerical modeling of the surface erosion occurring at a fluid/soil interface undergoing a flow process. Following a previous work [3], the balance equations with jump relations are used and a penalization procedure is used to compute Navier-Stokes equations around obstacles, with a fictitious domain method, in order to avoid body-fitted unstructured meshes. The water/soil interface evolution is described with a Level Set function coupled to a threshold erosion law. In order to allow adaptive mesh refinement, we develop a Discrete Duality Finite Volume scheme (DDFV). The ability of the model to predict the interfacial erosion of soils is confirmed by presenting several simulations.

**Keywords:** Interfacial erosion, Incompressible flow, Navier-Stokes, Fictitious domains, Discrete Duality Finite Volume, Adaptive mesh refinement, Level Set.

## 1 Introduction

Erosion phenomena is one of the main causes of the failure of hydraulic works such as dams, dykes and levees. In this context, the numerical modeling of the piping erosion of soil is a challenging problem [1], [2]. The model validated in [3] considers the erosion of a cohesive soil generated by a water flow tangential to the soil/water interface. The threshold erosion law is described by the shear stress of water at the soil/water interface. As the accuracy of the model depends strongly on the mesh discretization around the soil/water interface, adaptive mesh refinement is used, contrary to [3] where the mesh is a staggered cartesian grid. This obliges to use an adapted space discretization to Navier-Stokes equations, Discrete Duality Finite Volume scheme are chosen.

## 2 Physical model

The erosion model is described in [3], [4] and [5]. We consider an impervious soil under a diluted flow. With these assumptions, the solid/water interface can be considered as a sharp interface. As proved in [3], the time scales of the flow and of the erosion process are so different that the flow is described by the stationary Navier-Stokes equations at moderate Reynolds numbers. The velocity in the soil $\mathbf{u}_s$ is assumed to vanish and the soil/water interface $\Gamma$ is driven by the threshold law of erosion.

### 2.1 Governing equations

### Field equations

Let's denote $\Omega_f$ the fluid domain and $\Omega_s$ the soil domain. The fictitious domain approach, introduced by Angot in [10] and used by Golay *and al.* in [3], allows to describe the behavior of the two subdomains with a Navier-Stokes system defined on the whole domain $\Omega = \Omega_f \cup \Omega_s$:

$$\left\{ \begin{array}{rl} \rho(\partial_t \mathbf{u} - \mathbf{u} \wedge \mathrm{rot}(\mathbf{u})) - \mu\Delta\mathbf{u} + \nabla p = & \rho\mathbf{g} - \frac{\mu H}{K_s}(\mathbf{u} - \mathbf{u}_s), \\ \mathrm{div}(\mathbf{u}) = & 0, \\ (+\ \mathrm{B.C.}) & \end{array} \right. \tag{1}$$

Where $\mathbf{u}$ is the flow velocity, $p$ is the pressure, $\rho$ is the water density, $\mu$ is the dynamic viscosity and $\rho\mathbf{g}$ represents the gravity force. The penalization coefficient $K_s$ can be interpreted as a low permeability and $H$ is the characteristic function of the soil domain, which is unity within $\Omega_s$ and zero elsewhere. The boundary conditions ($B.C.$) closing the system are determined according to the considered problem.

### Erosion law

The erosion law is an experimental law, validated by S. Bonelli [1] and R. Fell [2], which describes the interface behaviour. This threshold law links the eroded mass and the shear stress of the flow:

$$\dot{m}_{er} = \begin{cases} K_{er}(\tau - \tau_c) & \text{if} \quad \tau > \tau_c, \\ 0 & \text{otherwise}, \end{cases} \tag{2}$$

where $\tau_c$ is the critical shear stress and $K_{er}$ is the kinetic coefficient of erosion ($K_{er} > 0$).
The tangential shear stress is given by : $|\tau| = \sqrt{(\mathbf{T}\cdot\mathbf{n})^2 - (\mathbf{n}\cdot\mathbf{T}\cdot\mathbf{n})^2}$, where $\mathbf{T} = -p\mathbf{I}_d + 2\mu\mathbf{D}(\mathbf{u})$ denotes the stress tensor, $\mathbf{D}(\mathbf{u})$ denotes the symmetric part of the velocity gradient and $\mathbf{n}$ denotes the normal unit vector of the interface $\Gamma$ oriented outwards from the flow.
Based on the above assumption, the interface velocity is defined as follows ($\rho_s$ is the soil density):

$$\mathbf{v}_\Gamma = \frac{\dot{m}_{er}}{\rho_s}\mathbf{n}. \tag{3}$$

# 3 Numerical modeling

### DDFV scheme

The DDFV methods can be seen as a generalisation of Marker and Cell (MAC) methods on Cartesian grids. A $2D$ and $3D$ DDFV scheme was proposed and tested in several studies. The one we implement is based on the versions developed by B. Andreinov in [6], Y. Coudiere and F. Hubert in [7], [8].

- **Meshes and notations**:

  The DDFV mesh is defined as a couple of dual meshes $\mathcal{M} = (\mathcal{T}, \mathcal{D})$, where $\mathcal{T}$ is a set containing cells of center $K$ and vertices $A$ and $\mathcal{D}$ is a diamond mesh, related to the faces $F$.

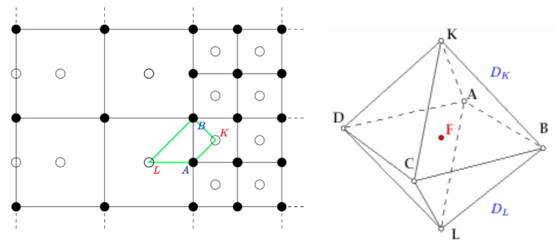


Figure 1: 2D DDFV mesh example and 3D diamond ($D_F = D_K \cup D_L$)

The velocity $\mathbf{u}^\mathcal{T}$ defined on $\mathcal{T}$ and the pressure $p^\mathcal{D}$ defined on $\mathcal{D}$ are respectively element of $(\mathbb{R}^3)^\mathcal{T}$ and $\mathbb{R}^\mathcal{D}$.

- **Discrete operators (3D)** :

  - The discrete gradient is a consistent approximation of the gradient operator of each component $u^\mathcal{T} = (u_K, u_L, u_A, u_B, u_C, u_D)$ of $\mathbf{u}^\mathcal{T} \in (\mathbb{R}^3)^\mathcal{T}$ and is defined by:

$$\nabla^\mathcal{D} u^\mathcal{T} = \frac{1}{3|D_F|}\left((u_L - u_K)\mathbf{N}_{KL} + (u_C - u_A)\mathbf{N}_{AC} + (u_D - u_B)\mathbf{N}_{BD}\right).$$

  - The discrete divergence is a consistent approximation of the divergence operator applied to the discrete tensor field $\mathbf{q}^\mathcal{D} \in (\mathbb{R}^3)^\mathcal{D}$ and is defined by :

$$\mathrm{div}^\mathcal{T}(\mathbf{q}^\mathcal{D}) = (\mathrm{div}_K(\mathbf{q}^\mathcal{D}), \mathrm{div}_A(\mathbf{q}^\mathcal{D}))_{K,A\in\mathcal{T}},$$

where $\mathrm{div}_K(\mathbf{q}^\mathcal{D}) = \frac{1}{|K|}\sum_{D\in\mathcal{D}} \mathbf{q}^\mathcal{D}\cdot\mathbf{N}_{KL}$, $\mathrm{div}_A(\mathbf{q}^\mathcal{D}) = \frac{1}{|A|}\sum_{D\in\mathcal{D}} \mathbf{q}^\mathcal{D}\cdot\mathbf{N}_{AC}$ and $\mathbf{N}_{AC}$ is a normal vector to an external surface of the control volume $A$ whose magnitude is this surface.

- **Global operators**:

  Thereafter, using the discrete operators $\nabla^{\mathcal{D}}$ and $\mathrm{div}^{\mathcal{T}}$ we are able to build several operators:

  $\mathrm{div}^{\mathcal{D}}\,\mathbf{u}^{\mathcal{T}} = \mathrm{tr}(\nabla^{\mathcal{D}}\,\mathbf{u}^{\mathcal{T}}) \quad \nabla^{\mathcal{T}}\,q^{\mathcal{D}} = \mathrm{div}^{\mathcal{T}}(q^{\mathcal{D}}\mathbf{I}_d) \quad \mathrm{rot}^{\mathcal{T}}\,\mathbf{q}^{\mathcal{D}} = \nabla^{\mathcal{T}} \wedge \mathbf{q}^{\mathcal{D}} \quad \triangle^{\mathcal{T}}\,\mathbf{u}^{\mathcal{T}} = \mathrm{div}^{\mathcal{T}}\,\nabla^{\mathcal{D}}\,\mathbf{u}^{\mathcal{T}}$

- **Discrete Green formula**:

  The discrete gradient and discrete divergence for a scalar-value function are linked by a discrete Green formula:

$$\left\langle \mathrm{div}^{\mathcal{D}}\,\mathbf{u}^{\mathcal{T}}, p^{\mathcal{D}} \right\rangle_{\mathcal{D}} = -\left\langle \mathbf{u}^{\mathcal{T}}, \nabla^{\mathcal{T}}\,p^{\mathcal{D}} \right\rangle_{\mathcal{T}} + \left\langle p^{\mathcal{D}}, \gamma^{\mathcal{D}}(\mathbf{u}^{\mathcal{T}} \cdot \mathbf{n}) \right\rangle_{\partial\Omega}, \tag{4}$$

  where $\gamma^{\mathcal{D}}$ is an adapted discrete trace operator. The notation $\langle \cdot, \cdot \rangle_X$ defined a scalar product on the space $X$.

- **Measure of errors and convergence orders**:

  The discrete operators divergence, gradient and curl are validated on evaluations of analytical functions. We compute the $L^2$ norms of the errors for different mesh sizes and found a convergence of order 2 in conformal and non conformal mesh.
  The validation of the Laplacian operator on the $\mathcal{T}$ mesh is obtained by solving $-\triangle^{\mathcal{T}}\,u^{\mathcal{T}} = f^{\mathcal{T}}$ with Dirichlet and Neumann boundary conditions. The discrete solution is compare to the analytical solution and shows a convergence with order 2. The Laplacian operator on the $\mathcal{D}$ mesh is also validated, we solve $-\triangle^{\mathcal{D}}\,p^{\mathcal{D}} = f^{\mathcal{D}}$ with homogeneous Dirichlet boundary conditions to obtain an order 2 convergence in conformal and non conformal mesh.

## Navier-Stokes discretization

A semi-implicit time discretization and a DDFV space discretization lead to the scheme in $\Omega$:

$$\left\{ \begin{array}{rl} \frac{\rho}{\delta t}(\mathbf{u}^{\mathcal{T}n+1} - \mathbf{u}^{\mathcal{T}n}) - \rho\mathbf{u}^{\mathcal{T}n+1} \wedge \mathrm{rot}^{\mathcal{T}}\,\mathbf{u}^{\mathcal{D}n} - \mu\,\triangle^{\mathcal{T}}\,\mathbf{u}^{\mathcal{T}n+1} + \nabla^{\mathcal{T}}\,p^{\mathcal{D}n+1} & \\ + \frac{\mu H}{K_s}(\mathbf{u}^{\mathcal{T}n+1} - \mathbf{u_s}^{\mathcal{T}}) = & \rho\mathbf{g}, \\ \mathrm{div}^{\mathcal{D}}\,\mathbf{u}^{\mathcal{T}n+1} = & 0, \\ (+\text{ B.C.}) & \end{array} \right. \tag{5}$$

where $\mathbf{u}^{\mathcal{T}n}$ and $p^{\mathcal{D}n}$ are respectively the velocity and the pressure at time $t_n = t\delta t$ on the DDFV mesh. Thanks to (4), the chosen time discretization (5) ensures an unconditionally $L^2$ stability property.
In order to deal with the implicit constraint of free divergence, we use a Projection method [9] to split the system. It is then necessary to solve a Poisson problem on pressure.

## Level Set method

The Level Set function $\phi$ [11], [12], defined as the signed distance to the interface soil/water describes the two media. The interface soil/water $\Gamma$ is represented by the zero level set of $\phi$. The displacement of the interface is driven by a transport equation:

$$\begin{cases} \partial_t\phi + \mathbf{v}_\Gamma^{ext} \cdot \nabla\phi & = 0 \\ \phi(x, t = 0) & = \phi_0, \end{cases} \tag{6}$$

where $\mathbf{v}_\Gamma^{ext}$ is an extension on the whole domain of the interface celerity $\mathbf{v}_\Gamma$ given previously in (3).

## The shear stress estimation

The penalized domain does not fit with the interface $\Gamma$. This induced an inaccurate shear stress computation at the interface. The inaccurate shear stress is limited to a four cells ($4h$) neighbourhood of $\Gamma$. It is then pertinent to compute the shear stress where the Level Set $\phi$ is close to $-4h$, corrected with the linear extrapolation (7) in order to evaluate it on $\Gamma$,

$$\tau^* = \tau - \phi \nabla\tau \cdot \frac{\nabla\phi}{\mid \nabla\phi \mid}. \tag{7}$$

The interface celerity is computed from $\mathbf{v}_\Gamma^* = \frac{K_{er}}{\rho_s}(\tau^* - \tau_c)$ and extended on the whole domain thanks to the following transport equation propagating the information from the region $\phi = -4h$,

$$\begin{cases} \partial_t \mathbf{v}_\Gamma^{ext} + H(\phi + 4h)\frac{\nabla\phi}{|\nabla\phi|} \cdot \nabla \mathbf{v}_\Gamma^{ext} & = 0, \\ \mathbf{v}_\Gamma^{ext}(x, t = 0) & = \mathbf{v}_\Gamma^*. \end{cases} \tag{8}$$

# 4 Validation

## Hole Erosion Test

We simulate the "Hole Erosion Test" as experimented by S. Bonelli, O. Brivois in [1], it is corresponding to an erosion by a poiseuille flow in an expanding cylindrical hole. We observe that our process increases the radius of the cylindcal domain. We compare the numerical simulation to the analytical solution developed by Bonelli and Brivois [6]. They propose the following law for the evolution of radius $r$, where $\triangle P$ denotes the imposed pressure gradient, $r0$ the initial radius and $L$ the length of the sample.

$$r(t) = \frac{2L\tau_c}{\triangle p} + (r_0 - \frac{2L\tau_c}{\triangle p})\exp(\frac{K_{er}\triangle p}{2L\rho_g}t)$$

We simulate an HET during $t_f = 0.45s$ and we compute the difference between numerical radius $r_{num}$ and analytical radius $r_{exc}$. We observe in the table below that the location of the interface, compare to that of the analytical solution, shows an order 1 convergence for the symmetrical distance of two sets of $\mathbb{R}^2$.
We define also a notion of radiality (measure of the distance from $\Gamma$ to the closer circle) and we find order 2 radiality of $\Gamma$ showing that the non body fitted mesh has minnor effect on accuracy.

| mesh size | $\parallel r_{num} - r_{exc} \parallel_\infty$ | radiality |
|---|---|---|
| $\frac{1}{10}$ | $1.96\ 10^{-2}$ | $8.87\ 10^{-3}$ |
| $\frac{1}{20}$ | $8.42\ 10^{-3}$ | $2.42\ 10^{-3}$ |
| $\frac{1}{40}$ | $4.06\ 10^{-3}$ | $6.51\ 10^{-4}$ |
| $\frac{1}{80}$ | $2.01\ 10^{-3}$ | $1.58\ 10^{-4}$ |

## Soil ball erosion

We consider a case of the erosion of a fixed ball of soil in a channel (Fig. 2). We impose a pressure gradient from the left to the right and a wall condition on the boundary except on the left and right (inflow and outflow) where a Neumann condition is imposed on velocity. We use an AMR mesh with a thin refinement around the ball. The Figure 2 shows the flow and the mesh restricted to a vertical cut.

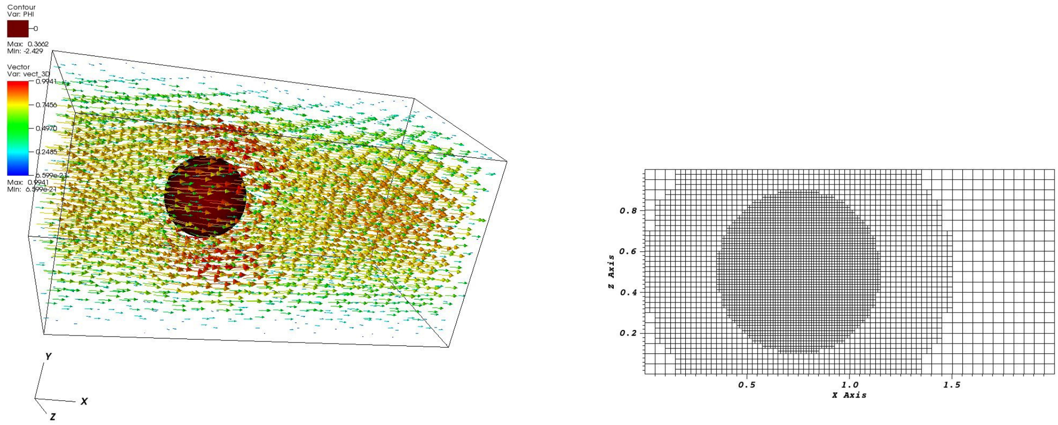


Figure 2: Ball under flow and AMR Mesh

The erosion of the ball is symmetric between inflow and outflow for the Stokes flow and similar to previous work of Golay *et al.* [5] . As expected and shown on Figure 3, the shear stress is the strongest in region close the lateral walls where the flow is increased.

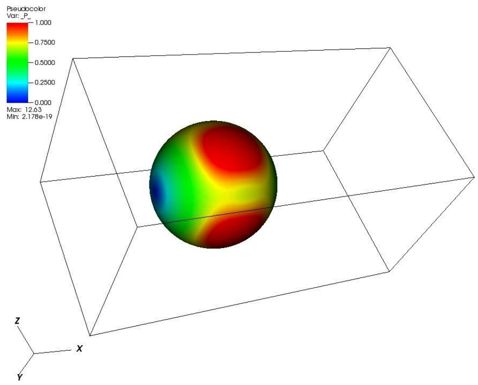


Figure 3: Shear stress on the ball for Stokes flow

# 5 Conclusion

The aim of this study was to draw up a numerical model for simulating interfacial erosion due to tangential flows. A unified model is introduced for the soil and the flow with the assumption of a diluted flow and sharp interface. A threshold erosion law, based on the shear stress, is devoted to the motion of the soil/water interface. The flow is driven by the Navier-Stokes equations. The soil layer is token into account thanks to a fictitious domain approach. The accuracy of the simulation induces the use of non uniform and non conformal meshes with thin meshes close to the interface. Then DDFV discretization has been developed as a generalization to Cartesian MAC grid for general meshes. A particular effort has been handled to compute accurately the shear stress at the interface. The water/soil interface evolution was described by a level set function. Several validation tests show a convergence of order 2 for the flow and order 1 for the erosion process. The relevance of the approach is illustrated by the simulation of the HET and 3D balls erosion.
Outgoing works will focus on the validation with respect to different laboratory experiments. And then in the case of higher Reynolds, we will analyze instabilities and fluctuations occurring during the erosion process. Finally, the aim is to couple water/soil erosion to air/water flows.

## References

[1] Bonelli S. & Brivois O.: The scaling law in the hole erosion test with a constant pressure drop *Int. J. Numer. Anal. Meth. Geomech.*, vol.32, pp. 1573–1595, (2008).

[2] Wan, C.& Fell ,R.: Laboratory Tests on the Rate of Pi- ping Erosion of Soils in Embankment Dams. *Journal of Geotechnical Testing Journal*, vol. 27, no.3. (2004)

[3] Golay, F., Bonelli, S., Lachouette, D. &. Seppecher, P: Numerical modelling of interfacial soil erosion with viscous incompressible flows. *Comp. Meth. In App. Mech. And Eng.*, vol.200, no. 1-4, 383-391, 2011.

[4] Bonelli, S., Golay, F., Lachouette, D. & Mercier, F.: Erosion of geomaterials. *Chapter 6, ISTE, Wiley*, ISBN 9781848213517, (2012).

[5] Golay, F., Lachouette, D., Bonelli, S. & Seppecher, P.: Interfacial erosion: a three-dimensional numerical model. *C.R. Mcanique*, vol.338, no. 6, pp. 333–337, (2010).

[6] Andreianov, B., Bendahmane, M., Hubert, F. & Krell, S.: On 3D DDFV Discretization of gradient and divergence operators. I. Meshing, operators and discrete duality. *IMA J. Numer. Analysis*, vol.32, no. 4, pp. 1574–1603, (2012) .

[7] Coudiere, Y., Hubert, F.: A 3D Discrete Duality Finite Volume method for nonlinear elliptic equations. *SIAM Journal on Scientific Computing*, vol.33, no. 4, pp. 1739–1764, (2011).

[8] Coudiere, Y. & Pierre, C.: A 2D 3D Discrete Duality Finite Volume Scheme. Application to ECG simulation. *International Journal on Finite Volumes*, vol.6, (2009).

[9] Guermond, J.L., Minev, P. & Shen, J.: An overview of projection methods for incompressible flows. *Comput. Methods Appl. Mech. Engrg.*, vol.195, no. 44-47, pp. 6011–6045, (2006).

[10] Angot, P., Bruneau, C.-H. & Fabrie, P.: A penalization method to take into account obstacles in incompressible viscous flowss. *Numer. Math.*, vol.81, pp. 497–520, (1999).

[11] Galusinski, C. & Vigneaux P.: On stability condition for bifluid flows with surface tension: application to microfluidics. *J. Comp. Phys.*, vol.227, no. 12, pp. 6140–6164, (2008).

[12] Osher, S. & Sethian, J.A. : Fronts propagating with curvature-dependent speed: Algorithms for tracking material interface. *J. Comp. Phys.*, vol.39, pp. 201–225, (1981).